Using the Special Sensor Microwave Imager to Monitor Surface Wetness

ALAN BASIST,* CLAUDE WILLIAMS JR.,* NORMAN GRODY,+ THOMAS F. ROSS,* SAMUEL SHEN,#
ALFRED T. C. CHANG,@ RALPH FERRARO,+ AND MATTHEW J. MENNE*

*National Climatic Data Center, NOAA/NESDIS, Asheville, North Carolina
+Atmospheric Research and Applications Division, Office of Research and Applications, NOAA/NESDIS, Camp Springs, Maryland
#Mathematics Department, University of Alberta, Edmonton, Alberta, Canada
@Hydrological Sciences Branch, Laboratory for Hydrospheric Processes, NASA Goddard Space Flight Center, Greenbelt, Maryland

(Manuscript received 1 February 2000, in final form 23 December 2000)

ABSTRACT

The frequencies flown on the Special Sensor Microwave Imager (SSM/I) are sensitive to liquid water near the earth's surface. These frequencies are primarily atmospheric window channels, which receive the majority of their radiation from the surface. Liquid water near the surface depresses the emissivity as a function of wavelength. The relationship between brightness temperatures at different frequencies is used to dynamically derive the amount of liquid water in each SSM/I observation at 1/3° resolution. These data are averaged at 1° resolution throughout the globe for each month during the period of 1992–97, and the 6-yr monthly means and the monthly anomalies of the wetness index are computed from this base period. To quantify the relationship between precipitation and surface wetness, these anomalies are compared with precipitation anomalies derived from the Global Precipitation Climate Program. The analysis was performed for six agricultural regions across six continents. There is generally a good correspondence between the two variables. The correlation generally increases when the wetness index is compared with precipitation anomalies accumulated over a 2-month period. These results indicate that the wetness index has a strong correspondence to the upper layer of the soil moisture in many cultivated areas of the world. The region in southeastern Australia had the best relationship, with a correlation coefficient of 0.76. The Sahel, France, and Argentina showed that the wetness index had memory of precipitation anomalies from the previous months. The memory is shorter for southeastern Australia and central China. The weakest correlations occurred over the southeastern United States, where the surface is covered by dense vegetation. The unique signal, strengths, and weaknesses of the wetness index in each of the six study regions are discussed.

1. Introduction

There are numerous potential applications of surface wetness observations throughout the globe. For instance, surface wetness is an important parameter for radiation models, because it affects the amount of energy used in latent versus sensible heat flux (Rind 1984). Agricultural interests need to identify soil moisture availability for crop growth and to monitor the development of a drought or a flood in an area (Ross 1999). Hydrologists need to know the amount of water in a basin and how streamflow will be affected by rainfall and snowmelt (Seth et al. 1999) to determine how much water is available for electricity generation, irrigation, or municipal water supplies. Because in situ observations of soil moisture are frequently too sparse to provide the adequate information (Robock et al. 2000), we investigated how a satellite-derived surface wetness index corresponds to precipitation. This relationship was analyzed under various conditions and for different regions of the world.

Unfortunately, it is very difficult and expensive to monitor the magnitude of surface water across a region, much less throughout the world. Large variations in climate and soil types across a region can introduce a tremendous amount of variability in precipitation and/or water retention characteristics at the surface. Therefore, point measurements at one location are not always representative of the surrounding area. Consequently, an integrated measurement over an area, such as satellite observations, can be extremely useful. In recognition of the strength of the above statements, there have been numerous studies on the correspondence of satellite observations with surface wetness (Basist et al. 1998; Verhoest et al. 1998; Lakshmiet et al. 1997).

This article investigates the utility of using microwave frequencies to monitor the magnitude of liquid water near the surface and attempts to identify whether a significant part of the microwave signal received by the Special Sensor Microwave Imager (SSM/I) comes from the upper level of the soil. It is widely known the

Corresponding author address: Alan Basist, National Climatic Data Center, 151 Patton Ave., Rm. 120, Asheville, NC 28801.
E-mail: abasist@ncdc.noaa.gov

microwave frequencies used in this study cannot penetrate a dense vegetative canopy, which limits their ability to see the ground (Owe et al. 1992). As a result, it is difficult to determine what percentage of the signal comes from the vegetated canopy as compared with the ground below (Wang 1985). Even when the ground is exposed, the current theory indicates that frequencies flown on the SSM/I radiometers cannot penetrate more than a few centimeters below the surface, and therefore these measurements correspond more to pooling on the surface than to the soil moisture (Entekhabi et al. 1995). However, some empirical evidence indicate that the SSM/I signal may have deeper penetration depth when the ground is exposed to the sensor, such as for a cultivated field (Vinnikov et al. 1999). Therefore, this study will investigate the relationship between the wetness index and precipitation across various soil types, agricultural conditions, and climatic regimes. Moreover, it will also analyze the lagged correspondence between the wetness index and precipitation anomalies. This latter analysis will help to determine whether the wetness signal contains a memory of precipitation over an extended period of time and therefore has correspondence to actual soil moisture.

2. Methodology

Our study will focus on passive microwave observations using the SSM/I flown by the Defense Meteorological Satellite Program. The sensors used in this study are mounted on the *F11* and *F13* satellites. The dataset used in this study begins in January of 1992 and continues through 1997. The frequencies observed by these sensors are 19, 22, 37, and 85 GHz, and all of these channels have dual polarization except for the 22 GHz, which receives only vertical polarization (Hollinger et al. 1987).

Surface water has a major impact on emissivity in the SSM/I spectrum (Prigent et al. 1997). Figure 1 demonstrates how water in the radiating surface (which may include vegetation and the upper level of the soil) influences the emissivity across the microwave frequencies. It shows theoretically derived spectral properties of a wet surface, for which emissivity drops in a direct response to water (Lakshmi et al. 1997). Specifically, the slope between the low and high frequencies directly responds to the amount of the radiating surface that is liquid water (Williams et al. 2000).

Basist et al. (1998) have developed an algorithm to observe surface wetness by measuring the change in surface emissivity relative to a dry surface. Once satellite measurements identify liquid water in the radiating surface (Williams et al. 2000), a dynamic emissivity correction is made to adjust for the lower emissivity of water. This emissivity correction is hereinafter referred to as the Basist Wetness Index (BWI), which takes the form of a linear relationship between channel measurements:

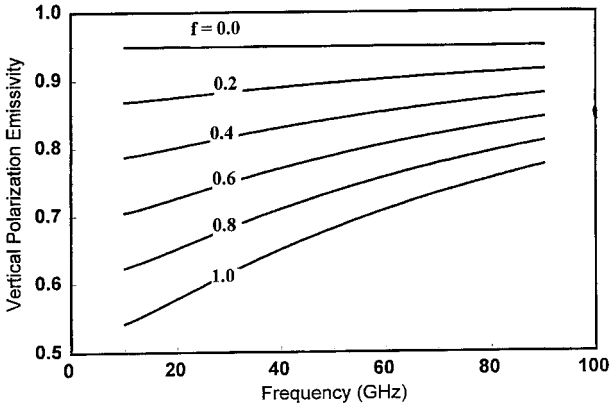

FIG. 1. A theoretical relationship of emissivity over a spectrum of microwave frequencies for six different magnitudes of surface wetness f. The top curve corresponds to 0% of the surface covered with water, and the bottom curve corresponds to 100% of the surface covered by water. Note how the slope of the curve changes as the fractional amount of surface water increases.

$$\text{BWI} = \Delta\varepsilon T_s = \beta_0[(T_b(\nu_2) - T_b(\nu_1)] + \beta_1[(T_b(\nu_3) - T_b(\nu_2)], \quad (1)$$

where $\Delta\varepsilon$ (change of emissivity) was empirically determined from SSM/I measurements, T_s is the actual surface temperature over a wet surface, T_b is the satellite brightness temperature for an SSM/I channel at frequency ν_n, and β_n is an empirically derived proportionality constant. The easiest way to explain the nature of BWI is to define it as the absolute difference between the 19-GHz channel measurement divided by 0.95 (the emissivity of dry ground) and the satellite-derived surface temperature. The magnitude of the wetness index ranges from 1 for marginally wet surfaces (such as dew in the canopy during the early morning hours) to values in excess of 40 (where a large portion of the radiating surface is inundated by water). These numbers correspond to the percentage of the radiating surface that is liquid water relative to a dry surface. Moreover, the denser the vegetation the more an observation is biased to the canopy.

The calibration of the proportionality constants in Eq. (1) was based on over 44 000 in situ temperatures T_s observed at the surface near the time of the satellite overpass. The best relationship used four of the satellites's channel measurements of (T_b) from an SSM/I observation. The majority of the weight (i.e., largest β term) corresponds to the 85V (vertical polarization) channel, because the emissivity of water is highest at this frequency. There is also significant weight given to 37H (horizontal polarization) which allows BWI to use the signal associated with polarization difference (Vinnokov et al. 1999). A histogram of the residuals (unexplained variance) between in situ–based and satellite-derived surface temperature is presented in Fig. 2. The differences between the observed (in situ based) and emissivity-adjusted (satellite derived) temperatures peak

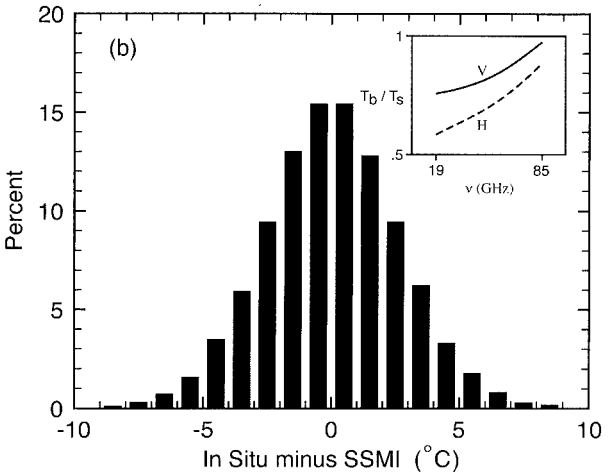

FIG. 2. The relationship between observed in situ and satellite-derived surface temperatures for wet conditions, based on 44 619 observations. The top-right-hand corner of the plot shows idealized signature of brightness temperatures along the SSM/I spectrum when a wet surface is observed. Note the slope of increasing emissivity as the frequency increases, along with the rapid decrease in polarization.

near zero and have an average error of 0.021°C, low standard deviation (2.64°C), and high symmetry (skewness is 0.066°C). As a consequence, temperature and wetness values are largely independent. The atmospheric contribution has also been minimized by the relationship between window and water vapor channels developed in the regression equation, although some residual errors may correspond to atmospheric conditions. [For a more complete description for the procedure of calculating the emissivity effect of water in the radiating surface, please refer to Williams et al. (2000).]

A map of the global BWI for July of 1997 is presented in Fig. 3. The index identifies the location of the intertropical convergence zone over northern Africa and shows the monsoonal areas in India and Southeast Asia. The major river basins around world (i.e., Amazon, Congo, Parana, and Mississippi) are evident. Note that the major tributaries of the Amazon are also observed, but the dense surrounding forest does not appear to be very wet, since the instrument cannot see through the dense canopy. Also, the irrigated region around numerous river valleys (i.e., Indus in Pakistan, Ganges in India, Red River in China) are clearly detected. The highest values tend to correspond to the tundra regions, where the snow cover has melted and water has pooled on the surface, since the permafrost below will not allow the water to percolate through the soil. Intermediate values of the index correspond to cultivated regions, while the areas with zero values correspond to the great deserts around the world.

The BWI is calculated independently for both morning and afternoon overpasses at the pixel (1/3°) resolution. Calculation of the monthly climatologies products from the daily observations of the SSM/I instrument is described in detail by Ferraro et al. (1996). Pixel values are averaged to 1° resolution for each month during the period 1992–97, allowing us to calculate a 6-yr climatology for each month of the year at 1° resolution. Then anomalies are derived for each month over the 6-yr base period. These anomalies are compared with an independent dataset [i.e., Global Precipitation

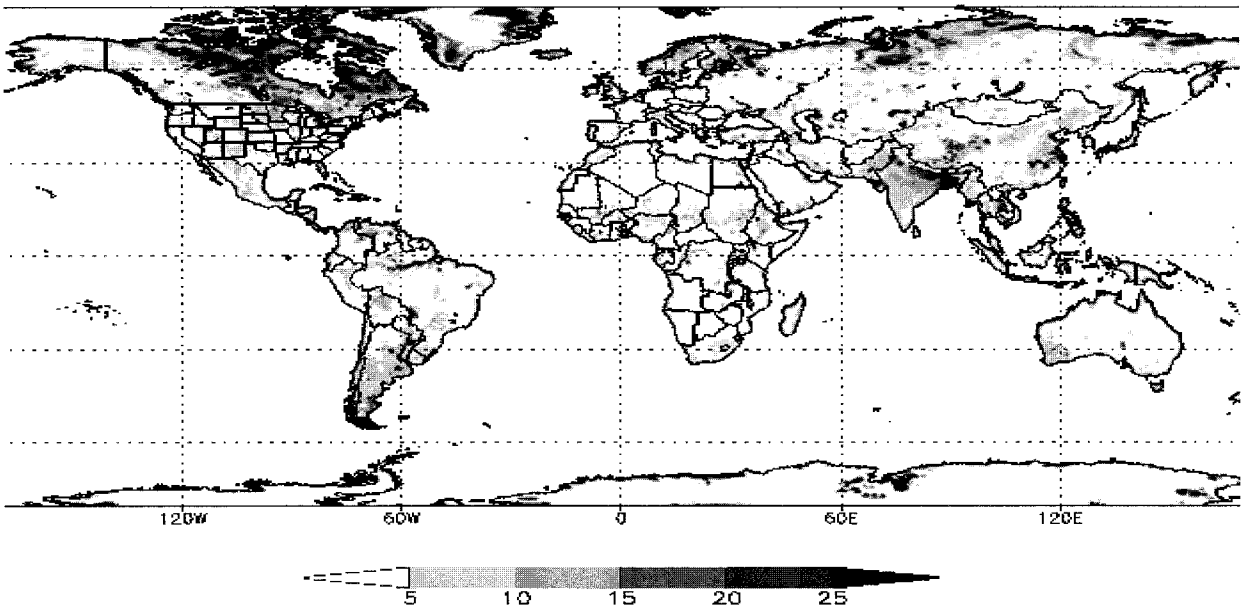

FIG. 3. A map of the BWI for the globe during Jul 1997. Note the high values in the tundra, wetlands, and broad river valleys. The moderate values correspond to areas for which the radiating surface contains some water, and zero values correspond to the major desert regions or dense vegetation that hides the ground.

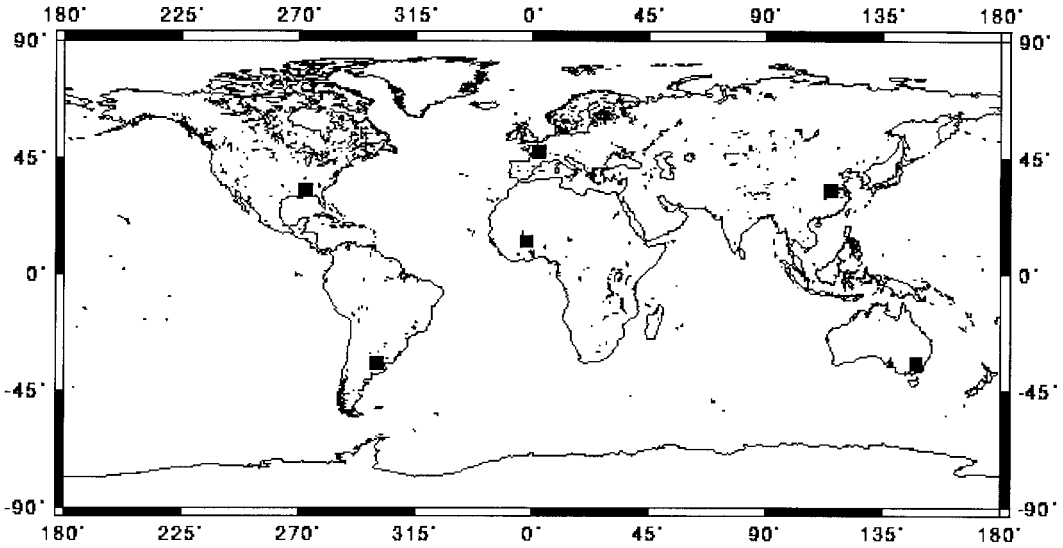

FIG. 4. A global map depicting the six study regions, each on a separate continent.

Climate Program (GPCP; Huffman et al. 1995)] to determine the strengths and weaknesses of BWI.

The GPCP precipitation values have been compiled over the same 6-yr period, thereby allowing for a direct comparison of their anomalies over the same base period. The GPCP values are derived from in situ point measurements, as well as infrared and microwave observations. The final product uses an interpolation scheme to produce global fields at 2.5° monthly resolution. Where in situ data are available, they get considerably more weight than satellite observations. Therefore, the comparison is made over areas where in situ observations were adequate to dominate the final GPCP product, thereby allowing us to substantiate the assumption that the two datasets are largely independent. A comparison of the two monthly anomalies provides a venue to validate the capacity of BWI as a proxy for upper-level soil moisture over an area.

3. Results

The following six sections correspond to a study region from around the globe (Fig. 4). Each section contains

1) the location of a 5° × 5° study area (this dimension is chosen to correspond with an atmospheric spatial scale of homogeneous conditions; Entin et al. 2000);
2) a description of the region's background climate, general soil types, and land cover (Matthews 1983);
3) the relationship between BWI and regional GPCP monthly anomalies for 1992–97; and
4) the statistical correlation of their relationship over time, as well as a description of the mechanisms influencing the strengths or weaknesses of the relationship.

a. Southeastern Australia

Southeastern Australia, defined here as the region within 32.5°–37.5°N and 145°–150°E, has a temperate climate that is frequently moist (Gentilli 1971). Temperatures average near 10°C in the winter and near 20°C in the summer. The study area contains the Great Divide mountain range, which exceeds 2000 m elevation at some isolated locations. Rainfall is generally greater on the east side of the study area, where annual precipitation averages near 600 mm, and diminishes to the west. Orographically enhanced precipitation can occur on both the east and west slopes of the mountains (Basist et al. 1994). Precipitation is fairly evenly distributed throughout the year, with a slightly higher concentration in the summer. The primary soil type is alfisol, with a gray to brown surface horizon and clay accumulation below the surface. This region is one of the most important agricultural areas in Australia, where wheat, corn, and oats are grown in abundance. A large portion of the land is grazed by sheep and cattle. The eastern section contains significant tracts of temperate hardwoods. The western section is the head water for one of the most important river basins on the continent, the Murray River, where water is stored in numerous reservoirs for various purposes.

Figure 5 shows the time series for wetness and precipitation anomalies during the period of 1992–97. In general, the wetness anomalies were slightly larger than the precipitation anomalies, and the two time series generally follow each other. The strong correspondence between these datasets is illustrated by a correlation coefficient of 0.76 (Table 1). Relative to the precipitation anomalies, the wetness anomalies tend to be more persistent from month to month. The largest difference between the two fields occurs in August and December of

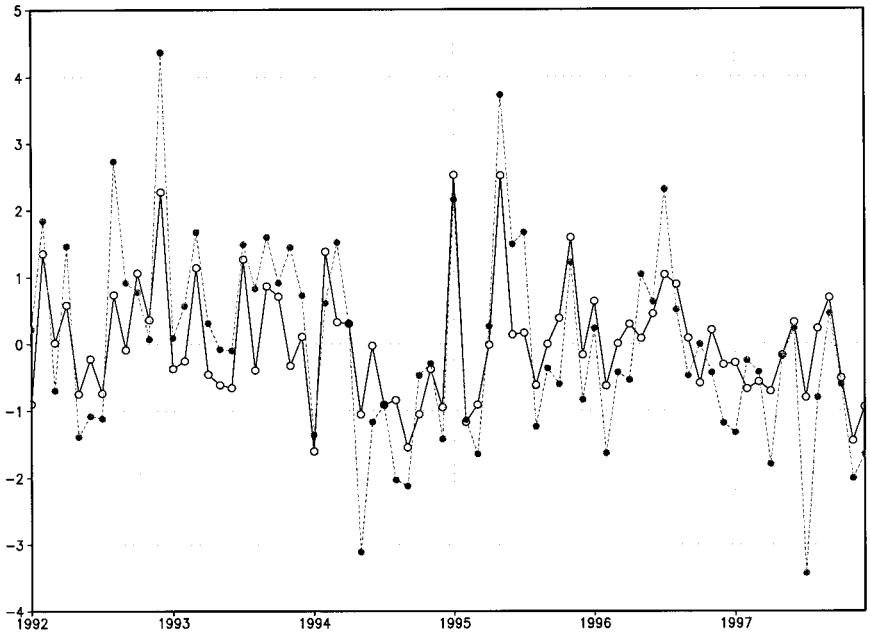

FIG. 5. A time series of the SSM/I-derived surface wetness (dashed) and GPCP-derived precipitation (solid) monthly anomalies for southeastern Australia (32.5°–37°5S, 145°–150°E) over the period of 1992–97. Units for the precipitation anomalies are in millimeters per day, and surface wetness index is unitless.

1992, May of 1994, and July of 1997. Ample rain and cooler than normal temperatures during both August and December of 1992 kept the upper level of the soil excessively moist. Furthermore, the extreme wetness in December kept the equipment from harvesting the crop, causing it to ferment in the field (CPC 1992–97, Vol. 79). In contrast, during May of 1994 the negative wetness anomaly was nearly 3 times the precipitation value. At this time, the CPC (1992–97, Vol. 81) stated that the top soil moisture was very low and that above normal temperatures further exacerbated the dry conditions, which delayed the planting and germination of the wheat crop. Last, during July of 1997 drought conditions and freezing temperatures (when water is in a frozen state it is not detected as wetness) kept the surface wetness anomalies at the lowest values of the study period (CPC 1992–97, Vol. 84).

TABLE 1. Correlation coefficients. Asterisk indicates that the relationship is significantly different from zero at the 99.9% level; two asterisks indicate significance at the 99.0% level. Bold values represent the highest correlation between the anomalies for the given region.

Region	Current month only	2 months of accumulation	3 months of accumulation
Southeastern Australia	**0.76***	0.64*	0.59*
Central France	0.46*	**0.62***	0.61*
Northern Argentina	0.53*	0.69*	**0.74***
Western Sahel	0.65*	**0.66***	0.64*
Central China	**0.62***	0.59*	0.56*
Southeastern United States	0.30**	**0.39***	0.36*

b. Central France

We compared the anomalies over central France (45°–50°N, 0°–5°E), where the major crops include wheat, grapes, oats, barley, sugar beets, fruit trees, and grazing land. It is a humid mesothermal climate associated with west-coast marine conditions. Soil type varies from inceptisol in the south, which is an immature weakly developed structure composed of a thin light-colored surface layer with little organic material, to alfisol in the north, which is a more mature surface layer, composed of brown-gray material with clay accumulates in the subsurface. This northern soil retains moisture better and is richer in organics. Annual precipitation in the region averages between 600 and 800 mm. The mountains in the southern section have an orographic influence, allowing some upslope areas to receive over 1200 mm, while downwind areas receive less than 500 mm. Precipitation is fairly evenly distributed throughout the year over this region. There is a distinct north-to-south temperature gradient, in which the mean temperature in July ranges from 17°C in the north to over 20°C in the south. January mean temperature averages between 5° and 8°C (Wallen 1970). The diurnal temperature range is moderate (9°C) to the north, and considerably higher (12°C) to the south. The entire area experiences freezing temperatures and snow cover, but extended periods below freezing are uncommon.

The year 1992 (Fig. 6) began with an exceptionally low wetness anomaly, which was a response to a deficit of precipitation from the preceding months (CPC 1992–97, Vol. 79). This deficit was also reflected in the fact

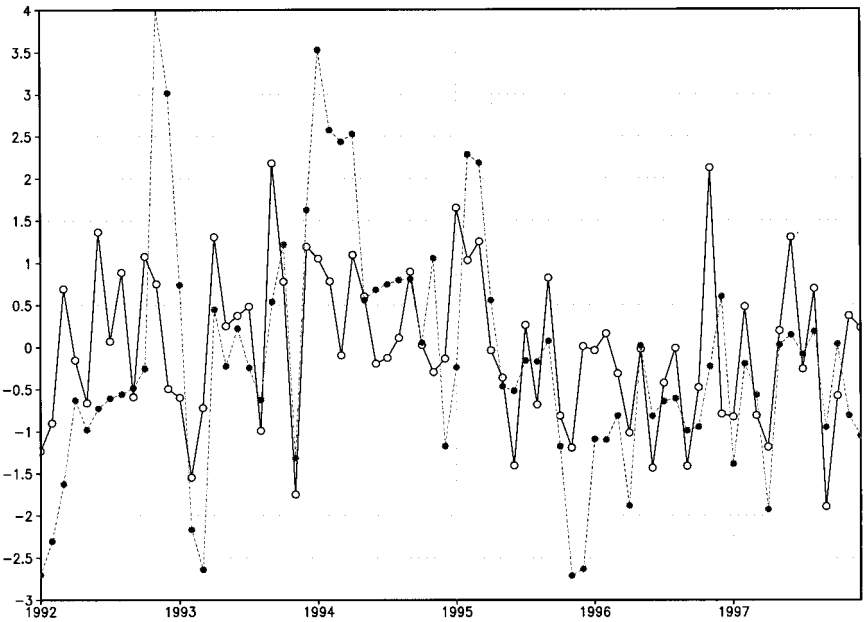

FIG. 6. The same as Fig. 5, but for central France (45°–50°N, 0°–5°E).

that the wetness anomaly took most of the year to reach positive values, while the precipitation anomalies fluctuated around the zero values. It is also evident that the wetness anomalies generally have a higher amplitude than precipitation. Furthermore, the highest values of the wetness anomalies consistently correspond to a prolonged period or above- or below-average precipitation. This aspect will be discussed in more detail in the following section. The correlation coefficient between concurrent anomalies is 0.46 across the time series (Table 1).

The largest discrepancies between the precipitation occurred in November and December of 1992, the first few months of 1994, November and December of 1995, and November of 1996. During late October and November of 1992, the excessive surface moisture stopped equipment from harvesting corn (CPC 1992–97, Vol. 79). At the beginning of 1994, soils were completely saturated, and above-average precipitation and cool conditions of winter allowed the excessive moisture to linger into the remaining months (CPC 1992–97, Vol. 81). During the last two months in 1995, dry conditions and below-freezing temperatures produced some of the lowest wetness anomalies over the study period. The last half of November of 1996 followed an extended dry period, and the excessive rains gave the region much-needed soil moisture.

c. Northern Argentina

Northern Argentina (37°–32°S, 63°–58°W) is an extremely important source of food for much of the world. The region grows wheat, corn, oats, millet, potatoes, flaxseed, and soybeans. There is also significant dairy farming in the region. The soil is mollisol (chestnut brown) with a rich organic surface, and the natural vegetation is grass. The precipitation across the region averages near 1000 mm a year and is slightly drier to the west. Rainfall is most abundant in summer and is lowest in winter, and the seasonality increases toward to the west. Temperatures average near 21°C in the summer and near 10°C in the winter (Schwerdtfeger 1976). The soil rarely dries out altogether, but it is also rarely saturated. A extended period of below-freezing temperatures or snow cover is unusual in this area.

In contrast to the wetness values, there is very little variability in the precipitation anomalies. The precipitation anomalies rarely exceed 2, whereas the wetness values commonly exceed 4 (Fig. 7). The largest wetness anomalies consistently occur in the latter part of extended wet and dry periods, which supports the perspective that this index has memory. We will discuss this point further in the following paragraph as well as the next section. The correlation coefficient between concurrent anomalies is 0.53 for the period of record (Table 1).

The biggest difference in the two variables occurred from April to October of 1994 (late winter). During this period, the precipitation anomaly averaged above the mean. The wetness values best reflected the trend at the end of the rainy period, when the surface was flooded and field work was delayed. An extended dry period during the midyear in 1995 produced an accumulative response in the wetness anomalies. At this time, it was noted that crops were stressed and the germination of winter wheat was retarded. During the first part of 1996, the precipitation anomalies rose above average, and wetness values responded by moving up toward the average

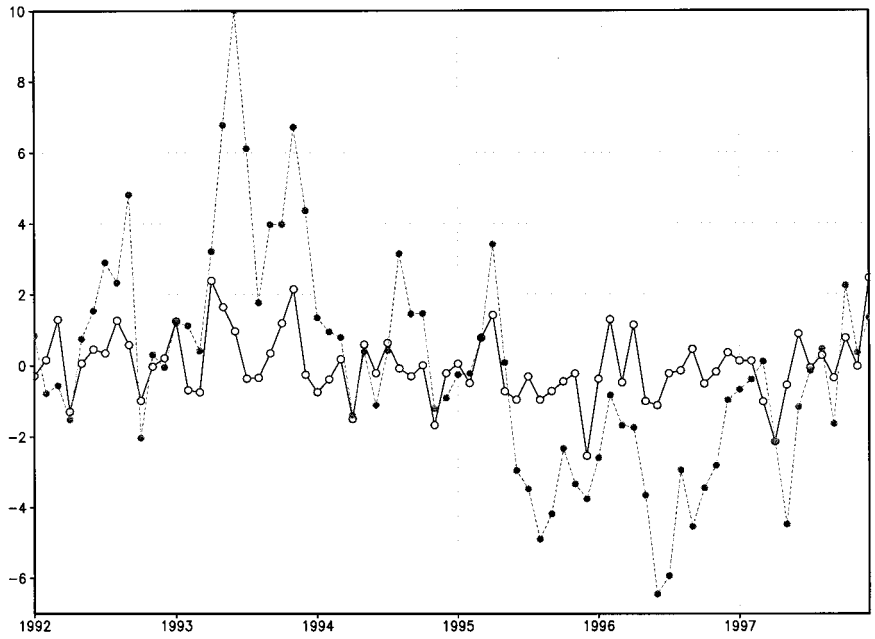

FIG. 7. The same as Fig. 5, but for northeastern Argentina (37°–32°S, 63°–58°W).

value. However, in May and June (as the precipitation once again went below the mean), the wetness anomalies dropped to their lowest values. At this time, the topsoil was so deficient of moisture that the winter crop did not emerge (CPC 1992–97, Vol. 83).

d. Western Sahel

The region in the western Sahel (10°–15°N, 5°W–0°) has a distinct monsoon climate. The summer wet season supports grazing land, millet, sorghum, peanuts, soybeans, corn, and cotton. The soil type is primary alfisol, a gray-brown surface layer with clastic accumulates in the subsurface. The climate is semiarid, with the rainy season primarily restricted from June to September (Griffins 1972). Annual precipitation averages from 800 to 1200 mm, with a clear gradient of wetter in the south and drier to the north. The eight months from October to May generally account for less than 25% of the annual precipitation. The temperature pattern clearly places this region in the Tropics, with relatively little annual range and mean daily values that average near 25°C.

May of 1992 brought above-normal precipitation, which was clearly detected by the wetness anomaly (Fig. 8). Rainfall is usually sparse in May (the rainy season typically starts in June), and water is the limiting factor for vegetated growth in this area. Therefore, the vegetation got off to an early start and covered the surface well before it normally does. The consequence is depressed wetness anomalies during the following months (although precipitation remained above average), because the early vegetation cover obscured the satellite instrument from observing the surface. During the following three months, precipitation was below average while temperatures were above average, causing the wetness index to continue to plummet.

In contrast, the rainy season started later than average in 1993. As a consequence, when ample precipitation fell in July, the surface water was clearly visible to the satellite instrument, which amplified wetness signature above the expected value. The 1994 rainy season also got off to a slow start; however, in July the precipitation anomaly was extremely large. For reasons stated above, the wetness anomaly was amplified in July, whereas the following two months brought them into better alignment. Throughout the remainder of the study period there is generally good agreement between the datasets. The correlation coefficient between concurrent anomalies is 0.65 across the time series (Table 1).

e. Central China

The region in east-central China (30°–35°N, 112.5°–117.5°E) extends from the Yangtze River valley in the south to the Huang River valley to the north and a plateau in the west. Most this area is composed of fertile lowlands that are heavily cultivated. The soil type ranges from entisol, composed of alluvium that is usually moist, to mountain soils of widely varying compositions. The primary crops in this area are rice and cotton. Also, wheat, tea, millet, peanuts, and soybeans are extensively cultivated. Some of the land is used to raise pigs, cattle, bamboo, and other wood products. Precipitation in the area ranges from 1300 mm in the south to 700 mm to the north (Arakawa 1969). Precipitation is maximum in the summer, followed by autumn and

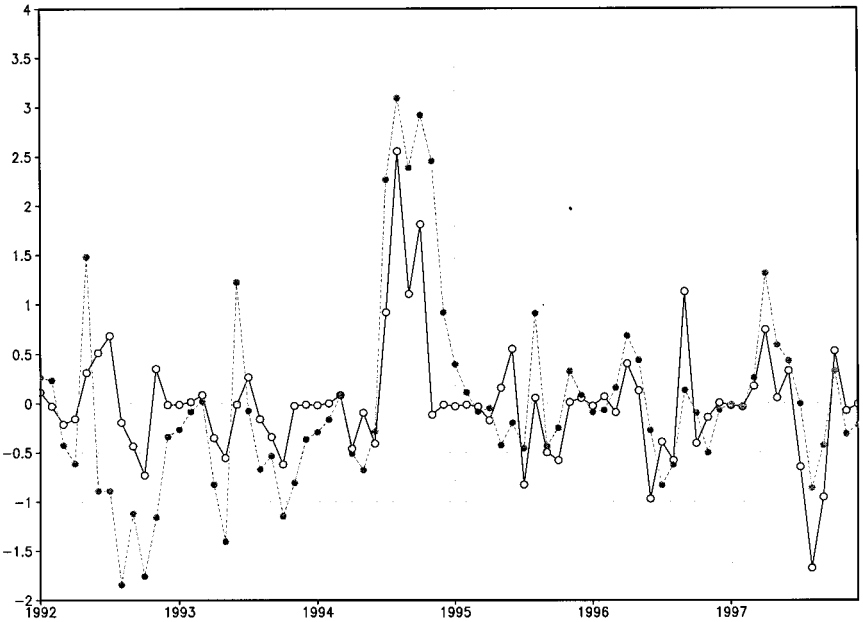

FIG. 8. The same as Fig. 5, but for western Sahel (10°–15°N, 5°–0°W).

spring, and the winter season receives less than 10% of the annual precipitation total. Snow covers the ground between 5 and 15 days of the year and is usually not very deep, although snowstorms do occasionally occur. Temperatures stay below freezing less than 15 days of the year. This area is classified as a continental climate, with hot summers and cool winters.

The two variables generally move together throughout the time series (Fig. 9), although the wetness values tend to have much higher anomalies, particularly at times when the precipitation values are anomalously below or above average for extended periods of time. The wetness index apparently responded to these periods by amplifying the anomalies in the direction of the persistent trend. We will discuss this issue more in the following section. When the two variables are correlated on a monthly timescale, the correlation coefficient is 0.62 (Table 1). Over this area of China, irrigation

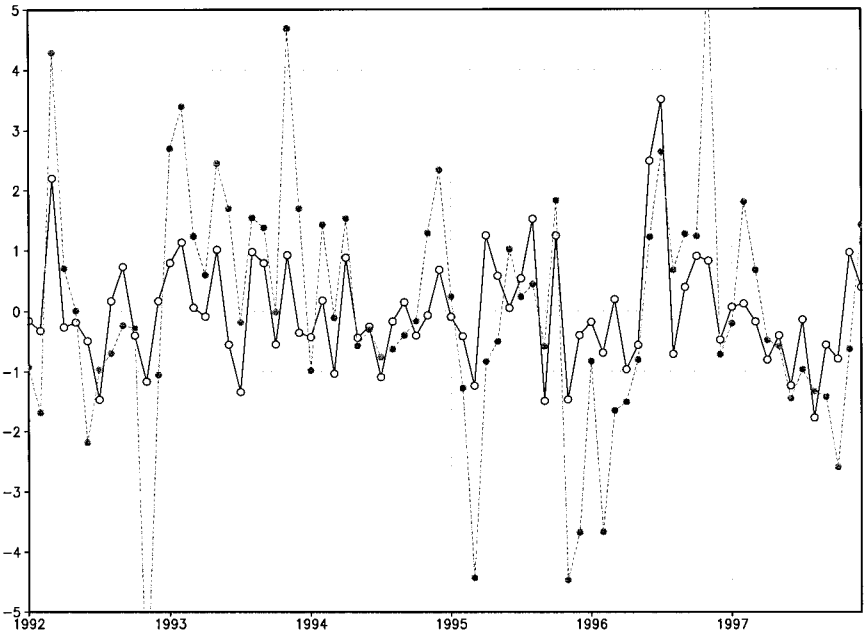

FIG. 9. The same as Fig. 5, but for south-central China (30°–35°N, 112.5°–117.5°E).

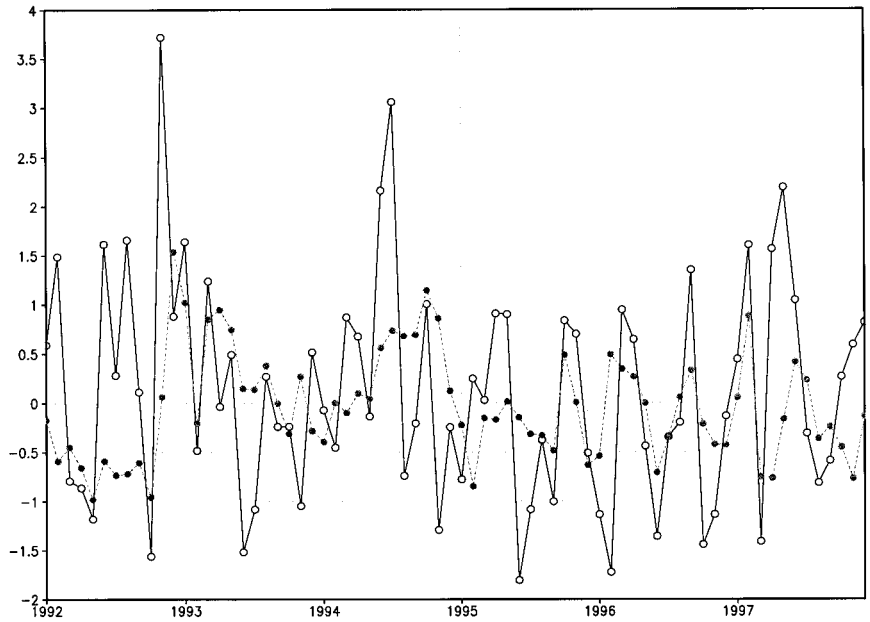

FIG. 10. The same as Fig. 5, but for the southeastern United States (30°–35°N, 90°–85°E).

of rice paddies can have considerable influence on the wetness index, and generally the source of this water does not come from precipitation inside the region. Therefore, the irrigated water adds noise to the relationship between precipitation and BWI.

There are appreciable outliers in the relationship between precipitation and wetness in Fig. 9. The largest of these occurred in November of 1992, when the wetness index was extremely low. CPC (1992–97, Vol. 79) states that precipitation was less than 50% normal and that rainfall deficiency upstream had significantly depleted the source of irrigation water for rice paddies at this time. In contrast, the wetness index was much higher than the precipitation anomaly in November of 1993. At this time, excessive rainfall (some areas received over 200% of normal amounts) and cool temperatures promoted localized flood and delayed planting of the second rice crop for the year. In March of 1995, the wetness anomaly was extremely low, following above-normal temperatures and much-above-normal precipitation for the second month in a row. The wetness index showed a dry period from November of 1995 to the spring of 1996; during this time, precipitation generally averaged less than 50% of normal expectations, while above-average temperatures increased the loss of surface moisture (CPC 1992–97, Vol. 83).

f. Southeastern United States

The region in the southeastern United States (30°–35°N, 90°–85°E) is subtropical and is frequently under the influence of moist tropical air from the Gulf of Mexico, which lies directly to its south. The region also receives winds from the west, which are usually mild and less humid. During the winter months, it experiences cold-air outbreaks from Canada, although these air masses are significantly modified by the time they reach this region. Annual precipitation across the area averages about 1300 mm per year. More than 100 days of the year in this area receive at least 0.25 mm, and about 35 of those days receive more than 35 mm, accounting for 80% of the total precipitation (Bryson and Hare 1974). On the average, there are 1–3 days per year with freezing precipitation, but it usually does not remain on the ground for more than a few days. Precipitation falls in significant quantities throughout the year, with the maximum concentration in the winter and spring and the lowest amounts in the late summer and early autumn. Annual temperature averages near 18°C, with slightly warmer conditions in the south. There is considerable seasonality; that is, winter temperatures average near 10°C, and summer temperatures average 27°C. Most of the region has utilisol soil, composed of subsurface clay accumulates, and the surface is usually moist and low in organic materials. The primary crops in the region are corn, soybeans, cotton, and pine trees.

The first feature to note on the time series is the low amplitude of the wetness anomalies, relative to the precipitation anomaly (Fig. 10). When the two variables are correlated on a monthly timescale, the correlation coefficient is 0.30. This relatively weak relationship is partially explained by the fact that much of the surface is covered by dense vegetation (pine trees and hardwoods) throughout the year, and by crops with a high leaf area index (corn and soybeans) throughout the growing season. This means that the satellite instrument gets much of its signal from the vegetative surface and not the ground. Another reason for the low correlation

over this region is the high frequency of precipitation events, which translates into low variability in surface water.

4. Memory retained by the BWI

Precipitation anomalies are aggregated over a period of months, and these aggregations were correlated with monthly values of BWI. This analysis will test the memory of the wetness index over a period of months and will investigate whether BWI retains signals from the upper reaches of the soil or is dominated by the signals from the surface. Theory states that SSM/I range of microwave frequencies does not penetrate more than 2 cm into the surface (Jackson 1993). However, models based on this theory may not accurately portray the penetration depth of these frequencies. An empirical study performed by Vinnikov et al. (1999) found that the SSM/I signal corresponds to the upper 10 cm of the soil. Our analysis empirically investigates this issue over various surface types and climatic conditions throughout the world. Our test is based on the assumption that water does not generally pool on the surface for extended periods of time; moreover, negative anomalies should not accumulate dryness (when the surface is dry it cannot get much drier). We expect that the unique features of each region should produce a unique set of results.

In four of the six study areas, correlations increased when the precipitation anomaly was aggregated between the previous and concurrent month. Two areas had the greatest rise in correlation: in France the correlation rose from 0.46 to 0.62, and in Northern Argentina it rose from 0.53 to 0.69. Moreover, in Argentina the correlation continued to rise to 0.74 when precipitation anomalies from the previous two months were aggregated with the contemporary month (i.e., a 3-month accumulated lag). Relative to the six study areas, these two study areas receive intermediate amounts of precipitation and have cultivation practices that expose a considerable portion of the soil to the satellite sensor. Figures 6 and 7 clearly display an accumulate response of BWI to trends in precipitation. When precipitation remained above or below average for several months in a row, the BWI had an accentuated signal in the same direction. Furthermore, when the precipitation anomalies shift from dry to wet conditions (or vice versa), BWI tended to lag behind the trend in precipitation, amplifying its response to precipitation anomalies during the second month of the trend. All of these empirical observations indicate that, under certain conditions, the BWI receives an appreciable portion of its signal from the soil and is not simply responding to surface conditions.

Over the southeastern United States, an accumulative lag produced a slight increase in the correlation. The correlation only rose from 0.30 to 0.39. This area is densely vegetated; therefore, an appreciable portion of this signal comes from the canopy, which clearly would not promote an accumulative response in the wetness index. We can postulate that the increase in the correlation is directly related to the portion of the signal that comes from the ground.

Over the western Sahel, the correlations remained similar between concurrent, 1-month, and 2-month accumulated lags. This area has a monsoon climate that tends to be either wet or dry. Therefore, the persistent nature of precipitation and its correspondence with the wetness index certainly influence the stable relationship over the various periods. Nonetheless, we associate part of the continuity in correlation with the fact that the soil accumulates moisture (dryness) over a period of months. The satellite is able to detect the signal, which indicates the memory of the wetness index. This is well demonstrated over the period of 1992–94, when the wetness index clearly lags in response to precipitation anomalies, both in the positive and negative tendencies.

One can question whether the increased correlation is an artifact of accumulative anomalies. Since precipitation tends to be a persistent parameter, that is, dry or wet months tend to follow each other, an accumulation of anomalies may increase the correlation. We tested this assumption by reversing the accumulative lag, allowing the precipitation to lag the wetness anomalies. When we ran these accumulative lags there was no instance when the correlation increased. Furthermore, the areas that had the largest accumulative increase in correlation (Argentina and France) experienced a rapid decrease in correlations when the reversed lag was implemented. These findings substantiate that the increased correlation is largely a physical signal of upper-level soil moisture and is not simply an artifact of increased correlation due to persistence.

5. Summary

This article presented the Basist Wetness Index derived from the microwave channels flown on the Special Sensor Microwave Imager. The surface emissivity at the SSM/I frequencies are depressed by liquid water in the radiating surface (which may include surface of the soil, canopy, and/or upper-level soil moisture). The magnitude of emissivity depression is related to the percentage of the radiating surface that is water. Furthermore, the emissivity depression is greatest at low frequencies, and the emissivity generally increases linearly at higher frequencies. As a consequence, brightness temperatures at the various frequencies can be used to identify the percentage of the radiating surface that is liquid water. This relationship was empirically derived using a linear correlation of in situ surface temperatures and concurrent satellite measurements.

We compared BWI directly with precipitation values provided by GPCP. Anomalies from both datasets were based on 1992–97. Analyses were performed over six regions of the globe, each corresponding to an agricultural area with spatial dimensions of $5^\circ \times 5^\circ$ on a dif-

ferent continent. The climate, soil, and vegetative cover were identified for each of these areas, in order for the reader to understand the unique nature of each region and how it affects the relationship between precipitation and BWI. Correlations between the two fields were based on monthly anomalies over the 6-yr period. The precipitation anomalies were also aggregated over multiple months to determine the memory of the BWI and its correspondence to upper-level soil moisture.

The correlation coefficients in Table 1 show that all the relationships between precipitation and wetness are positive and are significantly different from zero at the 99% confidence interval. Two (Australia and China) of the six study regions had their highest correlation when precipitation and BWI anomalies were concurrently compared. Three areas (France, Sahel, and the United States) had their highest correlation when precipitation anomalies were accumulated over a 2-month period. The remaining region (Argentina) had the highest value when precipitation anomalies were accumulated over a 3-month period. This discrepancy is largely a function of climatic conditions, soil type, vegetation cover, and land use. All six regions support major agriculture, but their land use affects the sensors' ability to detect a signal from the ground versus the canopy above. The land use ranges from monsoonal (Sahel), to irrigated (China), to largely cultivated (Argentina), to largely forested (southeastern United States). Moreover, soil type and climate influence the ability of the upper level of the soil to retain water over extended periods (Mattikalli et al. 1998).

Australia is the driest of the six regions, and its rainfall rarely exceeds the soil carrying capacity; therefore, water is likely to percolate downward or evaporate from the surface, leaving little memory of the precipitation in the upper level of the soil. The satellite instrument consequently receives a larger percentage of its signal near the time of the precipitation event, which is probably why the best relationship is concurrent. Moreover, a large percentage of this region is grassland for grazing, and includes forest cover in the mountains. Because this vegetative coverage is not tilled, the soil surface is not exposed to the satellite observations, further diminishing the ability of BWI to exhibit memory of precipitation from previous months.

In contrast, Argentina had its strongest correlation (0.74) when precipitation was accumulated over a 3-month period. Not surprisingly, its surface and climatic conditions are considerably different from Australia, although both regions grow wheat, corn, and oats. The vast majority of the Argentina study area is tilled, which readily exposes the soil to the satellite sensor. Moreover, precipitation is plentiful and distributed throughout the year. These features allow the upper level of the soil to retain moisture, effectively increasing the memory of the BWI.

There are three study regions in which the strongest correlation occurred when precipitation was accumulated over two months: France, Sahel, and the United States. The Sahel had the strongest correlation of the three regions ($r = 0.66$), followed closely by France ($r = 0.62$). Interestingly, in these regions, an intermediate percentage of the surface is cultivated, as compared with Australia at the low end and Argentina on the high end. Nonetheless, there are some notable climatic differences in the French and Sahel study areas. France is at a much higher latitude, where the vegetation demand for soil moisture is much lower. Although France is one of the driest study regions, its high latitude and cool temperatures promote a low evapotranspiration rate that allows the upper-level soil moisture to retain memory over an extended period. In contrast, the Sahel has a tropical climate with a distinct dry season for more than one-half of the year. During this time, the upper-level soil moisture is completely depleted and there is no memory, whereas during the rainy season, precipitation is generally abundant, and the memory of the soil moisture (observed by the satellite) extends for several months. As a consequence, the final best correlation between BWI and precipitation peaks with a 2-month accumulative lag for both of these regions.

Central China is very different from the other study regions, because rice cultivation is largely dependent on irrigation water. Moreover, the source of irrigation is generally outside the study region, which means the relationship between BWI and local precipitation breaks down. Much of central China is covered by a lush canopy of cultivated crops that limits the satellite's ability to observe soil moisture, and canopy interception is a primary source of signal for the BWI, which promotes the strong concurrent relationship between the two variables.

The region with the weakest correlation is the southeastern United States, where a dense forest cover dominates much of the area. This cover severely limits the ability of the satellite signal to penetrate below the canopy. Although the relationship between BWI and precipitation is weak, there apparently is enough signal from the cultivated areas that the highest correlations occur with precipitation accumulated over multiple months.

From these findings, one can conclude that BWI can be used to monitor the magnitude of water in the upper level of the soil. These results agree with findings of Vinnokov et al. (1999), who found that over Illinois soil moisture variations in the top 10 cm can be determined by microwave observations. Furthermore, Entin et al. (2000) found that the top 10 cm of soil moisture anomalies were not significantly different from anomalies within the top meter. Nonetheless, we demonstrated that correspondence between the BWI signal and soil moisture is greatly influenced by the climate, soil type, land use, and vegetative cover. The best relationship occurs over agricultural areas, where the tilled ground exposes an appreciable portion of the surface to the satellite sensor. Areas with large rainfall amounts and dense veg-

etative cover do not have as much variability in upper-level soil moisture, which means the interannual wetness signal is weaker. Conversely, a very dry environment does not show a strong signal, because the water quickly leaves the near surface. It appears that the best correspondence between precipitation and the BWI signals comes from agricultural areas, where the rainfall is sufficient to promote cultivation but is not heavy enough to saturate the ground for extensive periods. Even under these conditions, ancillary information allows for better interpretation of the BWI.

Acknowledgments. The authors thank editor Dara Entekhabi for his valuable comments, as well as the three anonymous reviewers who dedicated much time and effort to critically reviewing this article and who provided numerous suggestions that greatly improved the quality of the research and the final manuscript.

REFERENCES

Arakawa, H., 1969: *Climates of Northern and Eastern Asia.* Vol. 8, *World Survey of Climatology,* Elsevier Scientific, 248 pp.

Basist, A., G. D. Bell, and V. Meentemeyer, 1994: Statistical relationships between topography and precipitation patterns. *J. Climate,* **7,** 1305–1315.

——, N. C. Grody, T. C. Peterson, and C. N. Williams, 1998: Using the Special Sensor Microwave/Imager to monitor land surface temperatures, wetness, and snow cover. *J. Appl. Meteor.,* **37,** 888–911.

Bryson, R. A., and F. K. Hare, 1974: *Climates of North America.* Vol. 11, *World Survey of Climatology,* Elsevier Scientific, 420 pp.

CPC, 1992–97: *Weekly Weather and Crop Bulletin,* Vols. 79–84. [Available from Climate Prediction Center, W/NP52, NOAA/NWS/NCEP, 4700 Silver Hill Rd., Stop 9910, Washington, DC 20233-9910.]

Entekhabi, D., H. Nakamura, and E. G. Njoku, 1995: Solving the inverse problem for soil moisture and temperature profiles by sequential assimilation of multifrequency remotely sensed observations. *IEEE Trans. Geosci. Remote Sens.,* **32,** 438–448.

Entin, J. K., A. Robuck, K. Y. Vinnikov, S. E. Hollinger, S. Liu, and A. Namkhai, 2000: Temporal and spatial scales of observed soil moisture variations in the extratropics. *J. Geophys. Res.,* **105,** 11 865–11 877.

Ferraro, R. R., F. Weng, N. C. Grody, and A. Basist, 1996: An eight-year (1987–1994) time series of rainfall, clouds, water vapor, snow cover, and sea ice derived from SSM/I measurements. *Bull. Amer. Meteor. Soc.,* **77,** 891–905.

Gentilli, J., 1971: *Climates of Australia and New Zealand.* Vol. 13, *World Survey of Climatology,* Elsevier Scientific, 404 pp.

Griffins, J. F., 1972: *Climates of Africa.* Vol. 10, *World Survey of Climatology,* Elsevier Scientific, 604 pp.

Hollinger, J. R., B. Lo, G. Poe, R. Savage, and J. Pierce, 1987: Special Sensor Microwave user's guide. Naval Research Lab. Tech. Rep., Washington, DC, 119 pp.

Huffman, G. J., R. F. Adler, B. Rudolf, U. Schneider, and P. R. Keehn, 1995: Global precipitation estimates based on a technique for combining satellite-based estimates, rain gauge analysis, and NWP model precipitation information. *J. Climate,* **8,** 1284–1295.

Jackson, T. J., 1993: Measuring surface soil moisture using passive microwave remote sensing. *Hydrol. Processes,* **7,** 1139–1152.

Lakshmi, V., E. F. Wood, and B. J. Choudhury, 1997: Evaluation of Special Sensor Microwave/Imager satellite data for regional soil moisture estimation over the Red River Basin. *J. Appl. Meteor.,* **36,** 1309–1328.

Matthews, E., 1983: Global vegetation and land use. *J. Climate Appl. Meteor.,* **22,** 474–487.

Mattikalli, N. M., E. T. Engman, T. J. Jackson, and L. R. Ahuja, 1998: Microwave remote sensing of temporal variations of brightness temperature and near-surface soil water content during a watershed-scale field experiment, and its application to the estimation of soil physical properties. *Water Resour. Res.,* **34,** 2289–2299.

Owe, M., A. A. van de Griend, and A. T. C. Chang, 1992: Surface moisture and satellite microwave observations in semiarid southern Africa. *Water Resour. Res.,* **28,** 829–839.

Prigent, C., W. B. Rossow, and E. Matthews, 1997: Microwave land surface emissivities estimated from SSM/I. *J. Geophys. Res.,* **102,** 21 867–21 890.

Rind, D., 1984: The influence of vegetation on the hydrological cycle in a global climate model. *Climate Processes and Climate Sensitivity, Geophys. Monogr.,* No. 29, Amer. Geophys. Union, 3–91.

Robock, A., K. Y. Vinnikov, G. Srinivasan, J. K. Entin, S. E. Hollinger, N. A. Speranskaya, S. Liu, and A. Namkhai, 2000: The Global Soil Moisture Data Bank. *Bull. Amer. Meteor. Soc.,* **81,** 1281–1299.

Ross, T., cited 1999: Climate of 1999. [Available online at http://www.ncdc.noaa.gov/ol/climate/research/.]

Schwerdtfeger, W., 1976: *Climates of Central and South America.* Vol. 12, *World Survey of Climatology,* Elsevier Scientific, 532 pp.

Seth, A., R. C. Bales, and R. E. Dickenson, 1999: A framework for the study of seasonal snow hydrology and its interannual variability in the alpine regions of the Southwest. *J. Geophys. Res.,* **104,** 22 117–22 136.

Verhoest, N. E. C., P. A. Troch, C. Paniconi, and F. P. DeTroch, 1998: Mapping basin scale variability source areas from multitemporal remotely sensed observations of soil moisture behavior. *Water Resour. Res.,* **34,** 3235–3244.

Vinnikov, K. Y., A. Robock, S. Qui, J. K. Entin, M. Owe, B. J. Choudhury, S. E. Hollinger, and E. G. Njoku, 1999: Satellite remote sensing of soil moisture in Illinois, United States. *J. Geophys. Res.,* **104,** 4145–4165.

Wallen, C. C., 1970: *Climates of North and Western Europe.* Vol. 5, *World Survey of Climatology,* Elsevier Scientific, 252 pp.

Wang, J. R., 1985: Effects of vegetation on soil moisture sensing from an orbiting microwave radiometer. *Remote Sens. Environ.,* **17,** 141–151.

Williams, C., A. Basist, T. C. Peterson, and N. Grody, 2000: Calibration and validation of land surface temperature anomalies derived from the SSM/I. *Bull. Amer. Meteor. Soc.,* **81,** 2141–2156.